

L  
Lasers  
CL, P

# Longitudinal Mode Beat Intensities in a CW HF Chemical Laser

Prepared by C. P. WANG and R. L. VARWIG  
Aerophysics Laboratory

19 February 1976

Prepared for  
VICE PRESIDENT AND GENERAL MANAGER  
LABORATORY OPERATIONS

19980309 288



Laboratory Operations  
THE AEROSPACE CORPORATION

WASHINGTON D.C. 20301-7100  
7100 DEFENSE PENNACON  
BALLISTIC MISSILE DEFENSE ORGANIZATION  
BMD TECHNICAL INFORMATION CENTER  
BALISTIC MISSILE DEFENSE ORGANIZATION  
7100 DEFENSE PENNACON  
WASHINGTON D.C. 20301-7100

DTIC QUALITY INSPECTED  
DISTRIBUTION STATEMENT A

Approved for public release;  
Distribution Unlimited

U3996

## LABORATORY OPERATIONS

The Laboratory Operations of The Aerospace Corporation is conducting experimental and theoretical investigations necessary for the evaluation and application of scientific advances to new military concepts and systems. Versatility and flexibility have been developed to a high degree by the laboratory personnel in dealing with the many problems encountered in the nation's rapidly developing space and missile systems. Expertise in the latest scientific developments is vital to the accomplishment of tasks related to these problems. The laboratories that contribute to this research are:

Aerophysics Laboratory: Launch and reentry aerodynamics, heat transfer, reentry physics, chemical kinetics, structural mechanics, flight dynamics, atmospheric pollution, and high-power gas lasers.

Chemistry and Physics Laboratory: Atmospheric reactions and atmospheric optics, chemical reactions in polluted atmospheres, chemical reactions of excited species in rocket plumes, chemical thermodynamics, plasma and laser-induced reactions, laser chemistry, propulsion chemistry, space vacuum and radiation effects on materials, lubrication and surface phenomena, photo-sensitive materials and sensors, high precision laser ranging, and the application of physics and chemistry to problems of law enforcement and biomedicine.

Electronics Research Laboratory: Electromagnetic theory, devices, and propagation phenomena, including plasma electromagnetics; quantum electronics, lasers, and electro-optics; communication sciences, applied electronics, semiconducting, superconducting, and crystal device physics, optical and acoustical imaging; atmospheric pollution; millimeter wave and far-infrared technology.

Materials Sciences Laboratory: Development of new materials; metal matrix composites and new forms of carbon; test and evaluation of graphite and ceramics in reentry; spacecraft materials and electronic components in nuclear weapons environment; application of fracture mechanics to stress corrosion and fatigue-induced fractures in structural metals.

Space Sciences Laboratory: Atmospheric and ionospheric physics, radiation from the atmosphere, density and composition of the atmosphere, aurorae and airglow; magnetospheric physics, cosmic rays, generation and propagation of plasma waves in the magnetosphere; solar physics, studies of solar magnetic fields; space astronomy, x-ray astronomy; the effects of nuclear explosions, magnetic storms, and solar activity on the earth's atmosphere, ionosphere, and magnetosphere; the effects of optical, electromagnetic, and particulate radiations in space on space systems.

THE AEROSPACE CORPORATION  
El Segundo, California

Accession Number: 3996

Publication Date: Feb 19, 1976

Title: Longitudinal Mode Beat Intensities in a CW HF Chemical Laser

Personal Author: Wang, C.P.; Varwig, R.L.

Corporate Author Or Publisher: Aerospace Corporation, El Segundo, CA 90245 Report Number: ATR-76(8204)-2 Report Number

Assigned by Contract Monitor: SLL 80 132

Comments on Document: Archive, RRI, DEW

Descriptors, Keywords: Longitude Mode Beat Intensity Continuous Wave Hydrogen Fluoride Chemical Laser Tune Frequency Gain  
Saturation Coefficient Oscillate Mode Competition Pulsation

Pages: 00021

Cataloged Date: Dec 07, 1992

Document Type: HC

Number of Copies In Library: 000001

Record ID: 25445

Source of Document: DEW

Aerospace Report No.  
ATR-76(8204)-2

LONGITUDINAL MODE BEAT INTENSITIES IN A CW  
HF CHEMICAL LASER

Prepared by

C. P. Wang and R. L. Varwig  
Aerophysics Laboratory

19 February 1976

Laboratory Operations  
THE AEROSPACE CORPORATION  
El Segundo, Calif. 90245

Prepared for

VICE PRESIDENT AND GENERAL MANAGER  
LABORATORY OPERATIONS

LONGITUDINAL MODE BEAT INTENSITIES IN A CW  
HF CHEMICAL LASER

Prepared

Charles P. Wang  
C. P. Wang

R. L. Varwig  
R. L. Varwig

Approved

Harold Mirels  
Harold Mirels, Head  
Aerodynamics and Heat Transfer  
Department

W. R. Warren, Jr.  
W. R. Warren, Jr., Director  
Aerophysics Laboratory

## ABSTRACT

Longitudinal mode beat intensities in a free-running cw HF chemical laser have been investigated. A simple expression has been derived that describes the variation of beat intensity with tuning frequency. Experimental observations of the variation of beat intensity with tuning frequency in a HF chemical laser agree with the theoretical prediction.

#### ACKNOWLEDGMENT

The authors are indebted to Dr. Harold Mirels for many helpful discussions, and T. L. Felker for technical support.

## CONTENTS

ABSTRACT .....	v
ACKNOWLEDGMENT .....	vi
I. INTRODUCTION .....	1
II. THEORY .....	3
III. EXPERIMENTAL RESULTS .....	9
IV. CONCLUSIONS .....	17
APPENDIX: EXACT AND APPROXIMATE EXPRESSIONS FOR THE GAIN AND SATURATION COEFFICIENTS .....	19
REFERENCES .....	21

## FIGURES

1. Characteristic Shape of the Beat Intensity Distribution vs $\beta'$ and $\Omega$ .....	8
2. Block Diagram of the Experimental Apparatus .....	10
3. Oscilloscope Trace of a Single-Mode Laser Output Intensity vs Mode Frequency .....	12
4. Typical Two-Mode Laser Output Spectra Obtained by a Scanning Fabry-Perot Interferometer .....	13
5. Oscilloscope Trace of Beat Intensity vs Frequency $\Omega$ .....	14
6. Frequency Spectrum of Beat Signal .....	16

## I. INTRODUCTION

When two or more longitudinal modes oscillate in a laser, mode pulling, mode pushing, mode competition, locking, population pulsations, and related phenomena occur. These have been described by Lamb's semiclassical theory<sup>1</sup> and by various numerical computations.<sup>2-5</sup> Experimental observations of one or more of these phenomena have also been made on He-Ne<sup>3,6</sup> and other lasers.<sup>7-9</sup>

The cw HF chemical laser is a potential high-efficiency, high-power gas laser.<sup>10,11</sup> Its gain medium, however, is rather complex due to the nature of the chemical reaction, rotation-vibration transitions, medium nonuniformity, and mixed inhomogeneous-homogeneous behavior. Hence, it is important to examine the mode competition and mode-pulling behavior in a HF chemical laser. Furthermore, on the basis of the beat frequency between longitudinal modes and the mode-pulling effect in a high-gain medium, a new active frequency stabilization scheme was conceived.<sup>8</sup> Because of the strong mode competition, the key to the success of this new scheme is whether or not a steady beat signal can be obtained.

The results of a study of the longitudinal mode competition in a cw HF chemical laser are reported here. On the basis of Lamb's semiclassical theory, a simple expression is formulated to describe the effect of mode competition and to calculate the variation of beat intensity with tuning frequency. Experimental observations are also given of the Lamb dip, mode competition, mode pulling, beat frequency, and beat intensity in a cw HF chemical laser.

## II. THEORY

The basic equations of Lamb's semiclassical description of a multimode laser are<sup>1</sup>

$$\frac{dI_n}{dt} = 2I_n(a_n - \beta_{nn}I_n - \sum_{m \neq n} \theta_{nm}I_m) , \quad (1)$$

where  $I_n$  is the dimensionless intensity for mode  $n$ ,  $a_n$  is the net gain coefficient for mode  $n$ ,  $\theta_{nm}$  is the cross-saturation coefficient by mode  $m$ ,  $\beta_n$  is the self-saturation coefficient for mode  $n$ , and  $t$  is time. These coefficients  $a_n$ ,  $\beta_n$ , and  $\theta_{nm}$  are functions of population inversion, cavity loss, and upper- and lower-state decay rates and include spontaneous and collisional decay, Doppler width  $K_u$ , distribution of active medium in the resonator, difference frequency  $\nu_m - \nu_n$ , and location of the oscillation frequencies  $\nu_n$  with respect to line center  $\omega$ . Exact expressions for these coefficients have been given by Lamb<sup>1</sup> and by Sayers and Allen.<sup>2</sup>

For stationary states,  $dI_n/dt = 0$ . Then, Eq. (1) becomes

$$a_n - \beta_{nn}I_n - \sum_{m \neq n} \theta_{nm}I_m = 0 , \quad (2)$$

where  $a_n$  corresponds to the net single-pass unsaturated gain of mode  $n$ ,  $\beta_{nn}I_n$  is the decrease in that net gain due to saturation of the gain by mode  $n$ , and  $\theta_{nm}I_m$  is the decrease in the gain due to the saturation by mode  $m$ .

The frequency-determining equations, namely, the frequency shift of mode  $n$  caused by anomalous dispersion, have been derived by Lamb<sup>1</sup> and are not discussed here. This is because, for free-running lasers, phase relations between modes are random and, hence, can be ignored.

For single-mode oscillation, Eq. (2) is simply

$$I_n = \frac{a_n}{\beta_n} . \quad (3)$$

In an inhomogeneously broadened gain medium,  $I_n$  can be expressed as<sup>1</sup>

$$I_n = 8 \frac{\exp \left[ -(\omega - \nu_n)^2 / Ku \right] - N^{-1}}{\gamma_{ab} \left[ 1 + \frac{\gamma^2}{\gamma^2 + (\omega - \nu_n)^2} \right]} , \quad (4)$$

where  $N$  is the relative excitation, which is the ratio of average population inversion and population inversion at threshold,  $\gamma_{ab}$  is the spontaneous emission and inelastic collision contribution to decay of atomic dipole, and  $\gamma$  is the atomic dipole decay constant.

From Eq. (4), the cut-off frequency  $\omega_c$  can be obtained by letting  $I_n = 0$ :

$$\omega_c = \omega \pm Ku \sqrt{\ln N} , \quad (5)$$

and the dip condition can be obtained by letting  $d^2 I_n / d \nu_n^2 \geq 0$ :

$$N \geq 1 + 2 \left( \frac{\gamma}{Ku} \right)^2 . \quad (6)$$

For two-mode operation, the solution of Eq. (2) is

$$I_1 = \frac{a_1 \beta_2 - a_2 \theta_{21}}{\beta_1 \beta_2 - \theta_{12} \theta_{21}} ,$$

$$I_2 = \frac{a_2 \beta_1 - a_1 \theta_{12}}{\beta_1 \beta_2 - \theta_{12} \theta_{21}} . \quad (7)$$

Because all these coefficients are complicated functions of  $v_n$  and physical parameters of the gain medium, only numerical solutions were obtained earlier. These numerical solutions show rapid change in mode intensities with change in frequency because of strong mode competition. In order to gain some insight into Lamb's equations and to illustrate the physics of the mode competition effect, a simple model is formulated. Let

$$\beta = \sqrt{\beta_1 \beta_2} , \quad \theta = \sqrt{\theta_{21} \theta_{12}} ,$$

$$s = \frac{1}{2} \left[ a_1 \sqrt{\frac{\beta \theta}{\beta_1 \theta_{21}}} + a_2 \sqrt{\frac{\beta_1 \theta_{21}}{\beta \theta}} \right] ,$$

$$d = \frac{1}{2s} \left[ a_1 \sqrt{\frac{\beta \theta}{\beta_1 \theta_{21}}} - a_2 \sqrt{\frac{\beta_1 \theta_{21}}{\beta \theta}} \right] ,$$

$$\beta' = \beta/\theta .$$

Then,

$$I_1 I_2 = \frac{s^2}{\theta^2} \left[ \frac{1}{(\beta' + 1)^2} - \frac{d^2}{(\beta' - 1)^2} \right] \quad (8)$$

Now let the mode spacing be  $\nu_2 - \nu_1 = \Delta$  and the center frequency be  $1/2(\nu_1 + \nu_2) = \omega + \Omega$ , where  $\Omega = 0$  for mid-tuning, and  $\Omega$  varies between 0 and  $\Delta/2$ . Then, all the variable  $\beta$ ,  $\theta$ ,  $s$ , and  $d$  are functions of  $\Omega$  (see Appendix).

Because both  $s$  and  $\theta$  are nonzero, the condition for positive beat intensity  $I_1 I_2 \geq 0$ , is simply  $\beta' \leq \beta_-$  or  $\beta' \geq \beta_+$ , where  $\beta_- = (1 - d)/(1 + d)$ , and  $\beta_+ = (1 + d)/(1 - d)$ . In region  $\beta_- < \beta' < \beta_+$ , Eq. (8) is negative, and we set  $I_1 I_2 = 0$  because mode intensities  $I_1$  and  $I_2$  are positive quantities. If either  $I_1$  or  $I_2 = 0$ , Eq. (7) is no longer valid, and the single-mode solution Eq. (3) has to be used.

For the cw HF chemical laser studied here, both the ratio of the collision-broadened linewidth to the Doppler linewidth and the ratio of cavity intensity to saturation intensity are much smaller than one. Hence, in the range of interest,  $0 \leq \Omega \leq \Delta/2$ , all the variables  $s$ ,  $d$ ,  $\theta$ , and  $\beta'$  are nonzero and are monotonic functions of  $\Omega$ , except for  $d = 0$  at  $\Omega = 0$ . In general, these variables can be approximated by a second-order polynomial of  $\Omega$ . The asymptotic form of these variables and a numerical example are given in the Appendix. Both  $s$  and  $\theta$  vary less than 50% in the range  $0 \leq \Omega \leq \Delta/2$ .

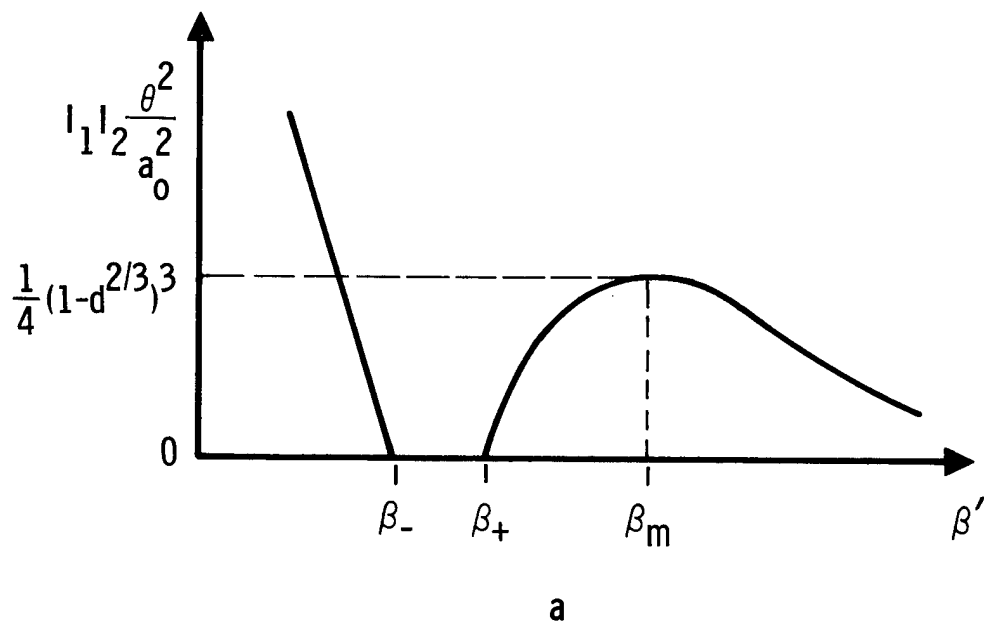
Because  $s$  and  $\theta$  are nonzero, monotonic, and slowly varying functions of  $\Omega$ , the locations of the maximum values of  $I_1 I_2$  and  $I_1 I_2 \theta^2/s^2$  are very close. Hence, in order to find the value of  $\Omega$  at which  $I_1 I_2$  is a maximum, we can let  $d(I_1 I_2 \theta^2/s^2)/d\beta' = 0$  and solve for  $\beta'$ . Since  $d < 1$ , we have only one real root:  $\beta_m = (1 + d^{2/3})/(1 - d^{2/3})$ . The maximum beat intensity at  $\beta_m$  is

$$\left( I_1 I_2 \frac{\theta^2}{s^2} \right)_{\beta'=\beta_m} = \frac{1}{4} (1 - d^{2/3})^3 \quad (9)$$

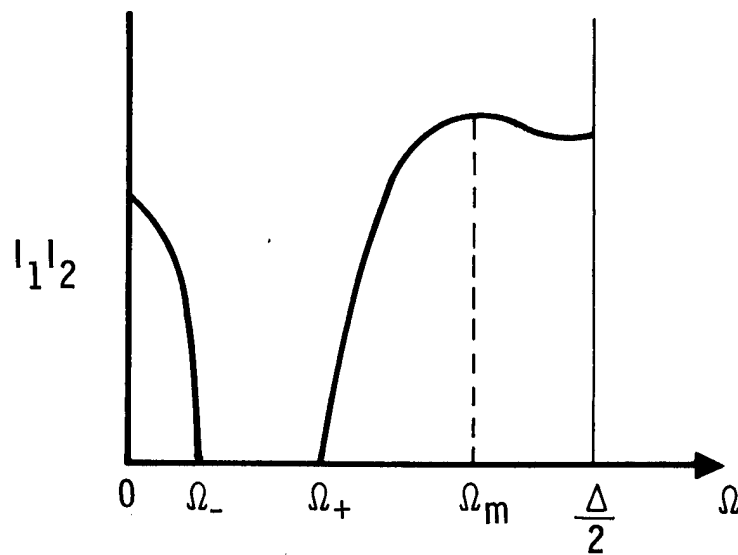
In an analysis of two-mode operation, Lamb<sup>1</sup> introduced a coupling parameter  $c \equiv \theta_{12} \theta_{21} / \beta_1 \beta_2$  and observed that the coupling is weak or strong as  $c < 1$ ,  $c > 1$ , respectively. Also, two-mode operation is unstable when  $c > 1$ . In terms of the present notation,  $c = (1/\beta')^2$ . We also note, from the definition of  $\beta_-$  and  $\beta_+$ , that  $\beta_- < 1$  and  $\beta_+ > 1$ .

The variation of beat intensity with  $\beta'$  is plotted in Fig. 1. In region  $\beta' < \beta_-$  i.e.,  $c > 1$ , the coupling is strong, and the lasing is unstable. In region  $\beta' > \beta_+$  i.e.,  $c < 1$ , the coupling is weak, and the lasing tends to be stable.

The variation of  $I_1 I_2$  with  $\Omega$  can be obtained by substituting the relation  $\beta' = \beta'(\Omega)$  into Eq. (8). Since  $\beta'$  can be approximated as a second-order polynomial of  $\Omega$ , the variation of beat intensity with  $\Omega$  is similar in Fig. 1a, except that the horizontal scale is shifted, stretched, or compressed nonuniformly. A typical plot is shown in Fig. 1b.



a



b

Figure 1. Characteristic Shape of the Beat Intensity Distribution vs  $\beta'$  and  $\Omega$

### III. EXPERIMENTAL RESULTS

In order to verify the theory, experiments were carried out with a cw HF chemical laser. The laser output spectra, beat frequencies, and beat intensities were measured by using a confocal scanning Fabry-Perot interferometer, spectrum analyzer, and fast InAs detector. The cw HF chemical laser used was described in an earlier paper.<sup>9</sup> Briefly, F atoms are generated by a discharge in a gas mixture of He, O<sub>2</sub>, and SF<sub>6</sub>. The latter is mixed with H<sub>2</sub>, which is injected just upstream of a transverse optical cavity. The cavity pressure could vary from 5 to 15 Torr. Typical single-line output at 2.87  $\mu$ m is 0.5 W. The gain medium is 10 cm long, and there is a small signal gain of about 0.05 cm<sup>-1</sup>.

A stable resonator was used that had a 2-m radius-of-curvature total reflector (reflectivity > 95%) and a flat grating (reflectivity 80%) as the output coupling. These were separated by distances of L = 30.6 cm and L = 162.6 cm for single-mode and two-mode operation, respectively. A TEM<sub>00</sub>-mode output beam was obtained by using a variable aperture inside the resonator. The total reflecting mirror was mounted on a PZT driver, which could move the mirror and scan the laser frequency across the gain linewidth. A schematic of the experimental arrangement is shown in Fig. 2.

In order to measure the beat frequency of the longitudinal modes, a room-temperature InAs detector with risetime less than 3 nsec was used. The beat signal was displayed on a Tektronix 7094 oscilloscope and analyzed by a Hewlett-Packard spectrum analyzer, model 8553B. A Burleigh 25-cm confocal scanning Fabry-Perot interferometer with free spectrum range of 300 MHz and resolution better than 5 MHz was used to analyze the laser output frequency spectrum. The laser and all the optics were mounted on a NRC vibration isolated table.

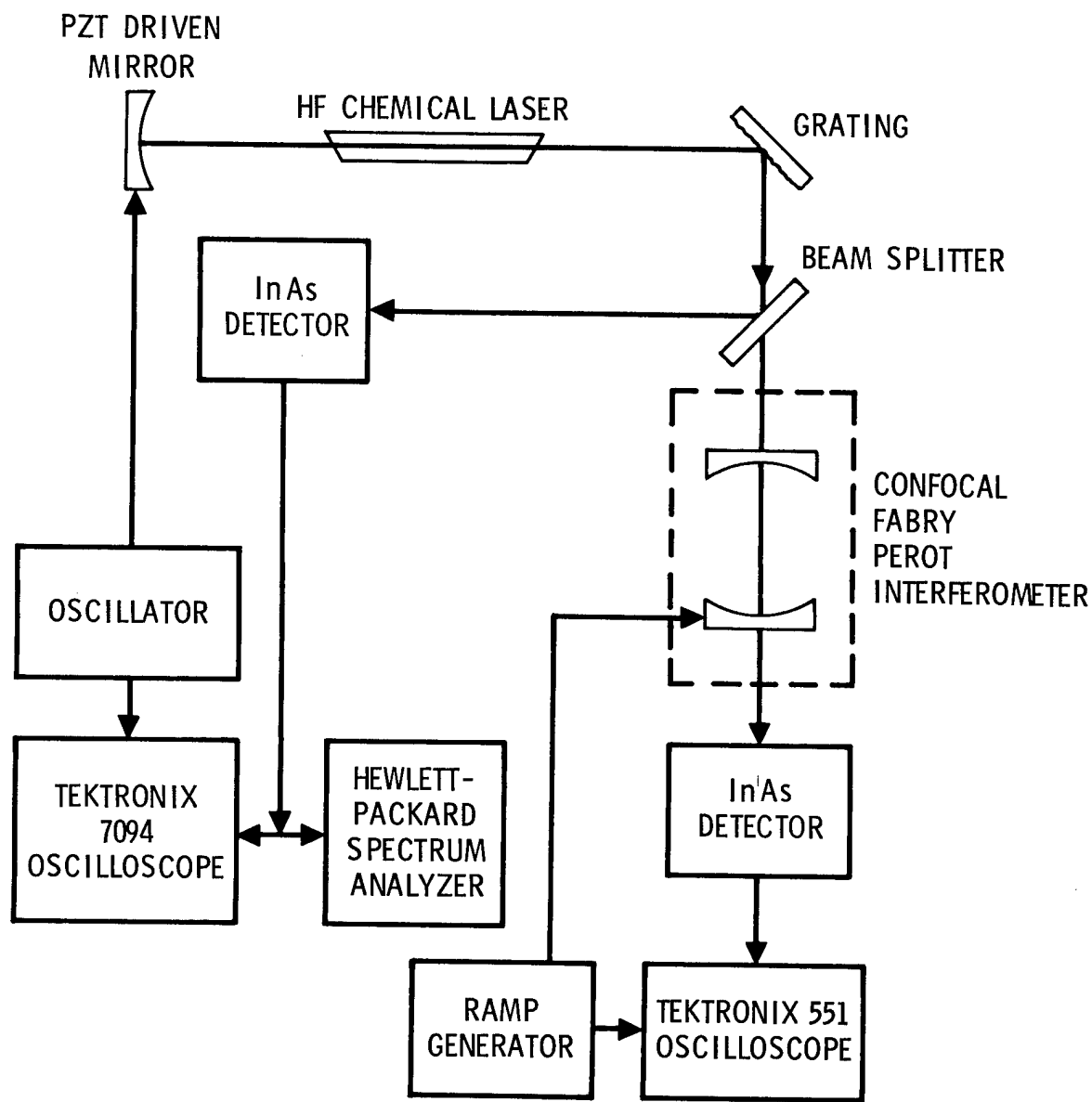


Figure 2. Block Diagram of the Experimental Apparatus

For single-mode operation, a cavity length  $L = 30.6$  cm was chosen. The empty cavity mode spacing is then 490 MHz, which is larger than the gain linewidth. The mode frequency can be continuously scanned through the gain linewidth by applying a high voltage on the PZT driver. A typical single-mode laser output intensity as a function of mode frequency is shown in Fig. 3. The Lamb dip in the center is clearly distinguishable, and the cut-off frequency can be determined. Similar Lamb dip was also observed in a HF chemical laser by Glaze.<sup>12</sup>

The saturation behavior results in the appearance of the Lamb dip [Eqs. (4) and (5)]. Its width is related to the radiative interaction width of individual molecules. Hence, information on collision effects can be obtained by investigating the pressure-dependent behavior of the dip.<sup>12, 13</sup>

For two-mode operation, a cavity length  $L = 162.6$  cm was chosen. The empty cavity mode spacing is then 92.3 MHz, which is much smaller than the gain linewidth. Hence, multimode operation can be achieved.

Typical laser output frequency spectra obtained by the scanning Fabry-Perot interferometer are shown in Fig. 4. The vertical scale is the laser intensity, and the horizontal scale is the frequency, swept at 28 MHz/div. The small bump in front of the peak is caused by a misalignment of the Fabry-Perot interferometer to reduce the coupling between the laser and the Fabry-Perot interferometer. Both traces were obtained by the same setup but were taken at 5 sec separation. The large variations of these two mode intensities indicate the strong mode competition effect.

A typical beat signal intensity distribution as a function of tuning frequency is shown in Fig. 5. The upper trace is the driving voltage of the PZT driver; the lower trace is the beat signal. Because of the low sweep speed, each individual oscillation of the beat signal can not be seen. However, the envelop, which is the beat intensity, is clearly discernable. The shape of the envelop agrees very well with the theoretical prediction (Fig. 1).

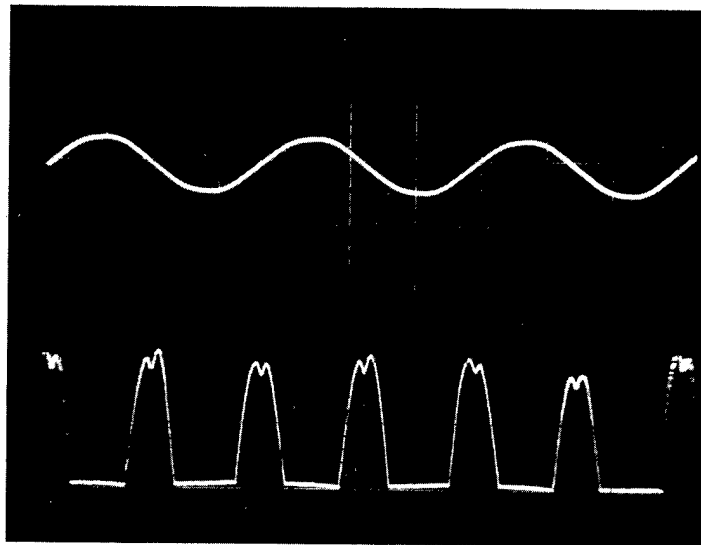


Figure 3. Oscilloscope Trace of a Single-Mode Laser Output Intensity vs Mode Frequency. Upper trace: driving voltage, 500 v/div, which is equivalent to 400 MHz/div. Lower trace: mode intensity, 200 mV div. Sweep speed, 5 msec/div.

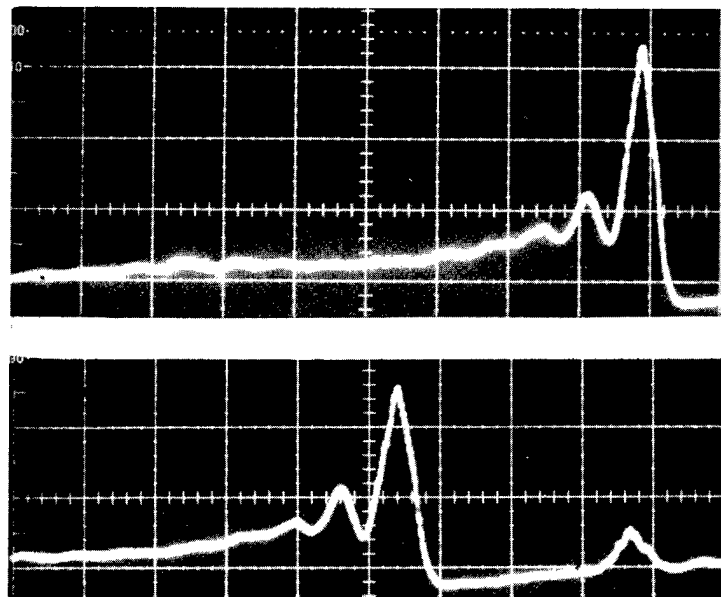


Figure 4. Typical Two-Mode Laser Output Spectra Obtained by a Scanning Fabry-Perot Interferometer.  
Vertical scale, 50 mV/div; horizontal scale, 28 MHz/div; sweep duration, 50 msec. Lower trace taken 5 sec after upper trace.

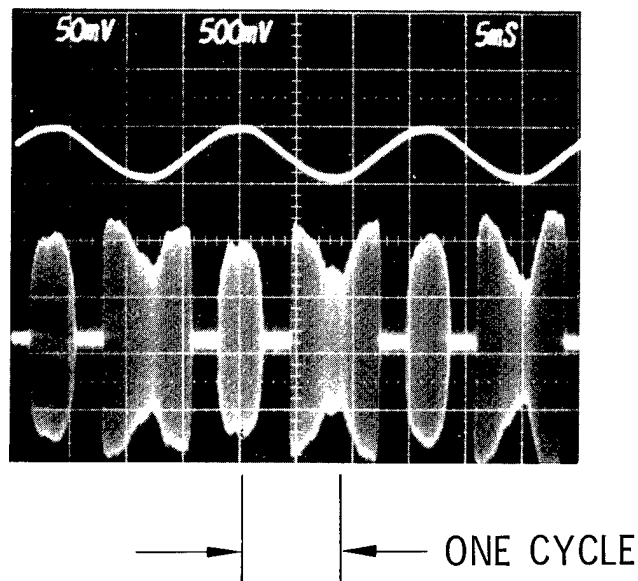


Figure 5. Oscilloscope Trace of Beat Intensity vs Frequency  $\Omega$ .  
Upper trace: driving voltage, 500 V/div, which is equivalent to 75 MHz/div. Lower trace: beat signal, 50 mV/div.  
Sweep speed, 5 msec/div.

For the beat frequency, two consecutive spectra with time separation of 2 sec are shown in Fig. 6. The center frequency was 88 MHZ, which agrees with Fig. 4. The beat frequency is smaller than the empty cavity mode spacing value of 92.3 MHz because of the mode pulling effect.<sup>7, 9, 14</sup> The width of the spectra is the result of a short-time (10 msec sweep duration) laser frequency instability, and the separation of these two spectra is the result of a long-time (2 sec separation) instability. On the basis of the theory developed in Ref. 9, these correspond to a short-time frequency instability of 10 MHz and a long-time (2 sec) frequency instability of 15 MHz. These agree with the results obtained by the scanning Fabry-Perot interferometer.

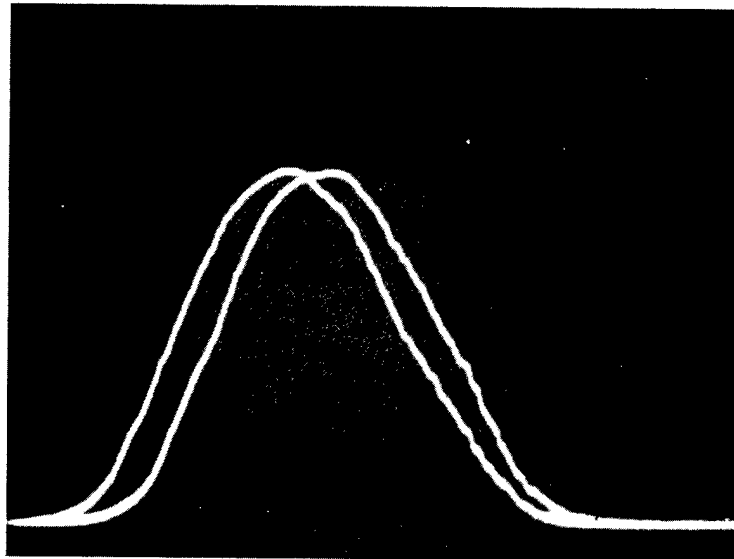


Figure 6. Frequency Spectrum of Beat Signal. Center frequency, 88 MHz; horizontal scale, 100 kHz/div; vertical scale, log intensity. Two consecutive sweeps separated by 2 sec are shown. Time duration for each complete sweep, 10 msec.

#### IV. CONCLUSIONS

A simple expression was obtained for variation of beat intensity with a parameter  $\beta'$ , which is a slowly varying function of the tuning frequency  $\Omega$ . This expression illustrates the general behavior of the beat intensity versus tuning frequency that results from mode competition effects. Furthermore, the results are useful for identifying regions of stable two-mode operation for use of active frequency stabilization of Ref. 9. Experimental observations are in good agreement with the theory.

APPENDIX: EXACT AND APPROXIMATE EXPRESSIONS  
FOR THE GAIN AND SATURATION COEFFICIENTS

Exact expressions for the coefficients from Ref. 1:

$$a_n = 4 \{ \exp[-(\omega - \nu_n)^2 / (Ku)^2] N - 1 \} F_3$$

$$\beta_n = [1 + \mathcal{L}(\omega - \nu_n)] F_3$$

$$\begin{aligned} \theta_{mn} = & \left[ \mathcal{L}\left(\omega - \frac{\nu_n}{2} - \frac{\nu_m}{2}\right) + \mathcal{L}\left(\frac{\nu_m}{2} - \frac{\nu_n}{2}\right) \right] F_3 \\ & + \frac{1}{2} \frac{\gamma_a \gamma_b \gamma}{\gamma_{ab}} \operatorname{Re} \left\{ [\mathcal{D}_a(\nu_m - \nu_n) + \mathcal{D}_b(\nu_m - \nu_n)] \right. \\ & \left. \times \left[ \mathcal{D}(\omega - \nu_n) \frac{N_2(m-n)}{N} + \mathcal{D} \frac{\nu_m}{2} - \frac{\nu_n}{2} \right] \right\} F_3 \end{aligned}$$

where  $\mathcal{L}(x) \equiv \gamma^2 / (\gamma^2 + x^2)$ ;  $\mathcal{D}_a(x) \equiv (\gamma_a + ia)^{-1}$ ;  $\operatorname{Re}$  is the real part;  $\nu_n$  is the laser frequency in mode  $n$ ;  $\gamma_a$ ,  $\gamma_b$  are upper and lower-level decay constants;  $\gamma_{ab} = 1/2(\gamma_a + \gamma_b)$ ;  $\gamma$  is the atomic dipole decay constant;  $\omega$  is the line center frequency;  $F_3 = (1/8)(\nu/Q_n)N$  is the third-order factor in laser coefficients;  $N$  is the relative excitation;  $N_2$  is the spatial Fourier component of the population inversion density;  $\nu/Q_n$  is the cavity bandwidth; and  $Q_n$  is the cavity quality factor for mode  $n$ .

The asymptotic form when  $\gamma_a$ ,  $\gamma_b$ ,  $\gamma < \Delta < Ku$ , and  $0 \leq \alpha \leq 1/2$  are:

$$\beta \simeq F_3 (A + B\alpha^2)^{1/2}$$

$$\theta \simeq F_3 (C + D\alpha^2)^{1/2}$$

$$s \simeq F_3 \left( E + \frac{\alpha}{N} \right)$$

$$d \simeq F_3 \frac{\alpha}{s} = \alpha \left( E + \frac{\alpha}{N} \right)^{-1}$$

where A, B, C, D, and E are constants of the order of one, and  $\alpha = \Omega/\Delta$ .

For a particular case when  $\gamma_a = \gamma_b = \gamma_{ab} = \gamma = \Delta/2$ ,  $N_2 = -1/2$ , and  $Ku = 2\Delta$ , we have, when  $\alpha = 0$ ,  $\beta = 1.32$ ,  $\theta = 1.45$ ,  $\beta' = 0.91$ ,  $A = 1$ ,  $s = 4$ , and  $d = 0$ ; and  $\alpha = 1/2$ ,  $\beta = 1.28$ ,  $\theta = 1.06$ ,  $\beta' = 1.20$ ,  $A = 0.93$ ,  $s = 4 + 1/2N$ , and  $d = 1/2 (4 + 1/2N)^{-1}$ . Hence,  $\beta$ ,  $\theta$ ,  $\beta'$ , and  $s$  are slowly varying functions of  $\Omega$  for  $0 \leq \Omega/\Delta \leq 1/2$ .

## REFERENCES

1. W. E. Lamb, Jr., Phys. Rev. 134, A1429 (1964); also, M. Sargent, III, M. O. Scully, and W. E. Lamb, Jr., Laser Physics (Addison-Wesley, Reading, Mass., 1974), Chaps. 9 and 10.
2. M. D. Sayers and L. Allen, Phys. Rev. 1A, 1730 (1970).
3. R. L. Fork and M. A. Pollack, Phys. Rev. 139, A1408 (1965).
4. V. M. Ermachenko and V. K. Matskevich, Sov. J. Quantum Electron. 4, 1115 (1975).
5. C. L. O'Bryan, III, and M. Sargent, III, Phys. Rev. 8A, 3071 (1973).
6. B. K. Garside, IEEE J. Quantum Electron. QE-4, 940 (1968).
7. L. Caspelson and A. Yariv, Appl. Phys. Lett. 17, 259 (1970).
8. C. P. Wang and S. C. Lin, J. Appl. Phys. 43, 5068 (1972).
9. C. P. Wang, J. Appl. Phys. 47, 221 (1976).
10. D. J. Spencer, H. Mirels, T. A. Jacobs, and R. W. Gross, Appl. Phys. Lett. 16, 235 (1970).
11. W. R. Warren, Jr., Acta Astronautica 1, 813 (1974).
12. J. A. Glaze, Appl. Phys. Lett. 23, 300 (1973).
13. T. Kan and G. J. Wolga, IEEE J. Quantum Electron. QE-7, 141 (1971).
14. J. J. Hinchen, J. Appl. Phys. 45, 1818 (1974).

## DISTRIBUTION

### Internal

R. A. Chodzko	H. Mirels
N. Cohen	D. A. Ross
D. A. Durran	D. J. Spencer
J. W. Ellinwood	S. N. Suchard
M. Epstein	D. G. Sutton
T. L. Felker	E. B. Turner
R. R. Giedt	R. L. Varwig
R. Hofland, Jr.	C. P. Wang
J. J. Hough	W. R. Warren, Jr.
M. A. Kwok	J. S. Whittier

### External

#### SAMSO

Lt. Col. Staubs (DYN)  
Lt. Col. J. R. Doughty (DYV)

#### AFWL

Kirtland AFB, NM 87117  
Col. R. Rose (AL)  
Dr. P. Avizonis (AL)  
Lt. Col. G. D. Brabson (ALC)  
Lt. Col. M. Bina (ALC)  
Maj. C. Forbrich (ALC)  
Dr. L. Wilson (ALC)  
Maj. D. Mitchell (DY T)

#### ARPA

1400 Wilson Blvd.  
Arlington, VA 22209  
Dr. P. Clark  
R. A. Moore

TRW Systems Group  
One Space Park  
Redondo Beach, CA 90278  
Dr. T. A. Jacobs  
Dr. G. Emanuel  
Dr. J. Miller 01/1080

CALSPAN Corporation  
P. O. Box 235  
Buffalo, NY 14221  
Dr. J. Daiber  
Dr. E. C. Treanor

Martin-Marietta  
Denver, CO 80202  
Dr. J. Bunting

AFRPL  
Edwards AFB  
Edwards, CA 93523  
B. R. Bornhorst (LKCG)

Naval Research Laboratory  
Code 6503, LTPO  
Washington, DC 20390  
Dr. W. Watt  
Dr. R. Airey  
Dr. J. M. MacCallum

Deputy Chief of Staff for  
Research, Development and  
Acquisition  
Dept. of the Army, Headquarters  
The Pentagon  
Washington, DC 20310  
Lt. Col. Benjamin J. Pellegrini/  
3B482

Los Alamos Scientific Laboratory  
Los Alamos, NM 87544  
Dr. K. Boyer  
Dr. R. Jensen  
Dr. G. Schott  
Dr. J. Parker  
Dr. E. Brock

AMSMI-RK  
Redstone Arsenal, AL 35809  
Dr. W. B. Evers, AMSMI/RK  
Dr. J. Hammond, AMSMI/RK  
Dr. W. Wharton, Bldg. 5452/RKL

AMSMI-RRP  
Bldg. 4762  
Redstone Arsenal, AL 35809  
Dr. T. A. Barr, Jr.

U. S. Naval Ordnance Lab.  
Silver Spring, MD 20910  
Dr. L. Harris  
Dr. D. Finkleman

NASA Ames Research Center  
Moffett Field, CA 94035  
Dr. C. F. Hansen  
Dr. H. Mark

Rocketdyne  
Canoga Park, CA 91304  
Dr. S. V. Gunn  
Dr. M. Constitine

Cornell University  
Dept. of Thermal Engr. / Lab. Plasma Phys.  
Ithaca, NY 14853  
Dr. T. A. Cool

Lockheed Palo Alto Research Lab  
Palo Alto, CA 94304  
Dr. W. C. Marlow

Lockheed Missiles and Space Company  
4800 Bradford Blvd.  
Huntsville, AL 35812  
J. W. Benefield

McDonnell Research Laboratory  
McDonnell Douglas Corporation  
St. Louis, MO 63166  
Dr. D. P. Ames  
Dr. R. Haakinen

Physics International Company  
2700 Merced Street  
San Leandro, CA 94577  
Dr. B. Bernstein

Massachusetts Institute of Technology  
Department of Physics  
Cambridge, MA 02139  
Dr. A. Javan

Mathematic Sciences Northwest, Inc.  
2755 Northrup Way  
Bellevue, WA 98004  
Dr. S. Byron  
Prof. A. Hertzberg

McDonnell Douglas  
5301 Bolsa Ave.  
Huntington Beach, CA 92647  
Dr. R. Lee/Bldg. 28, Rm. 250  
Dr. G. Berend/Bldg. 28, Rm. 250  
Dr. W. A. Gaubatz

Lawrence Radiation Lab.  
Livermore, CA 94550  
Dr. A. Karo  
Dr. J. Emmett

Arnold Engineering Development  
Center  
Arnold Air Force Station, TN 37389  
Lt. R. Case (XOOE)

AFWAL  
Wright-Patterson AFB, OH 45433  
Dr. K. Scheller  
Dr. J. Drewry

ESD (TRI)  
L. G. Hanscom AFB, MA 01731

AFCRL (OPL)  
Cambridge Research Laboratory  
Hanscom Air Force Base, MA 01730  
Dr. H. Schlossberg

AFSC (DLS)  
Andrews AFB  
Washington, DC 20331

AFML (SU)  
Wright-Patterson AFB, OH 45433

AFAL (CA)  
Wright-Patterson AFB, OH 45433  
Dr. B. List

Air University Library  
Maxwell AFB, AL 36112

Air Force Office of Scientific  
Research  
Bolling AFB, Bldg. 410  
Washington, DC 20332  
Directorate of Aerospace  
Sciences  
Directorate of Physics

FJSRL (Tech. Library)  
USAF Academy  
Colorado 80840

United Technologies Research  
Laboratories  
400 Main Street  
East Hartford, CN 06108  
Dr. D. Seery  
Dr. C. Ultee  
Dr. G. H. McLafferty

Hughes Research Laboratory  
3011 Malibu Canyon Road  
Malibu, CA 90265  
Dr. A. Chester

Avco-Everett Research Lab.  
2385 Revere Beach Parkway  
Everett, MA 02149  
Dr. G. W. Sutton  
Dr. J. Dougherty

Columbia University  
Dept. of Chemistry  
New York, NY 10027  
Dr. R. Zare

Science Applications, Inc.  
P. O. Box 328  
5 Research Drive  
Ann Arbor, MI 48105  
Dr. R. E. Meredith

Bell Aerosystems Company  
P. O. Box 1  
Buffalo, NY 14240  
Dr. W. Solomon

Northrop Corporation Laboratories  
Hawthorne, CA 90250  
Dr. M. L. Bhaumik

The RAND Corporation  
Via: AF Contracting Officer  
1700 Main Street  
Santa Monica, CA 90406  
Library - 98D  
for Dr. H. Watanabe

General Electric Company  
U7211 VFSTC  
P. O. Box 8555  
Philadelphia, PA 19101  
R. Geiger

Scientific and Technical Info.  
Facility (UNC)  
P. O. Box 33  
College Park, MD 20740 (A-Only)  
NASA Representative

RADC (SU)  
Griffiss AFB, NY 13442

NASA-Lewis Research Center  
21000 Brookpark Road  
Cleveland, OH 44135  
S. Cohen/M.S. 500-209

DDR&E  
Space Technology  
The Pentagon 3E139  
Washington, DC 20301  
Dr. R. A. Greenberg, Asst.  
Director

U. S. Army  
Advanced Missile Defense Agency  
1300 Wilson Blvd.  
Arlington, VA 22209  
Dr. M. Zlotnick, RDMD-NC  
Dr. L. Stoessel

U. S. Atomic Energy Commission  
Division of Military Applications  
Energy Resources Development  
Washington, DC 20301  
Dr. George W. Rhodes  
Dr. James McNally

Commander  
Naval Weapons Center  
China Lake, CA 93555  
Eric Lundstrom/Code 4011

Lockheed Missiles and Space Company  
P. O. Box 1103, West Station  
Huntsville, AL 35807

Dr. S. C. Kurzius  
Princeton University  
Dept. of Aerospace and Mech. Science  
Princeton, N. J.

Prof. S. Bogdonoff  
Purdue University  
School of Mechanical Engineering  
Chaffee Hall  
Lafayette, IN 47907

Prof. J. G. Skifstad  
California Institute of Technology  
Pasadena, CA 91109

Dr. A. Kuppermann  
Dr. H. Liepmann  
Dr. A. Yariv

University of Maryland  
College Park, MD 20740  
Dr. J. D. Anderson, Jr.  
Head, Dept. of Aerospace  
Engineering  
College of Engineering

Perkin-Elmer Corporation  
Norwalk, CO 06856  
M. L. Skolnick  
Electro-Optical Division

Dr. Walter R. Sooy  
SAI  
1651 Old Meadow Road  
McLean, VA 22101

Lincoln Laboratory  
Massachusetts Institute of Technology  
P. O. Box 73  
Lexington, MA 02173  
Dr. D. L. Spears